



Published in final edited form as:

*J Orthop Res.* 2018 July ; 36(7): 2052–2063. doi:10.1002/jor.23842.

## Effect of Connective Tissue Growth Factor Delivered Via Porous Sutures on the Proliferative Stage of Intrasynovial Tendon Repair

Stephen W. Linderman<sup>1,2</sup>, Hua Shen<sup>1</sup>, Susumu Yoneda<sup>1</sup>, Rohith Jayaram<sup>1</sup>, Michael L. Tanes<sup>3</sup>, Shelly E. Sakiyama-Elbert<sup>4</sup>, Younan Xia<sup>3</sup>, Stavros Thomopoulos<sup>5</sup>, and Richard H. Gelberman<sup>1</sup>

<sup>1</sup>Department of Orthopaedic Surgery, Washington University, 660 S. Euclid Avenue, Campus Box 8233, St. Louis 63110 Missouri

<sup>2</sup>Department of Biomedical Engineering, Washington University, St. Louis, Missouri

<sup>3</sup>Department of Biomedical Engineering, Georgia Institute of Technology, Atlanta, Georgia

<sup>4</sup>Department of Biomedical Engineering, University of Texas, Austin, Texas

<sup>5</sup>Department of Orthopedic Surgery, Department of Biomedical Engineering, Columbia University, 650 W 168 ST, Black Building 1408, New York 10025 New York

### Abstract

Recent growth factor, cell, and scaffold-based experimental interventions for intrasynovial flexor tendon repair have demonstrated therapeutic potential in rodent models. However, these approaches have not achieved consistent functional improvements in large animal trials due to deleterious inflammatory reactions to delivery materials and insufficient induction of targeted biological healing responses. In this study, we achieved porous suture-based sustained delivery of connective tissue growth factor (CTGF) into flexor tendons in a clinically relevant canine model. Repairs with CTGF-laden sutures were mechanically competent and did not show any evidence of adhesions or other negative inflammatory reactions based on histology, gene expression, or proteomics analyses at 14 days following repair. CTGF-laden sutures induced local cellular infiltration and a significant biological response immediately adjacent to the suture, including

---

Correspondence to: Richard H. Gelberman (T: 314-747-2531; F: 314-747-2599; gelberman@wudosis.wustl.edu). Correspondence to: Stavros Thomopoulos (T: 212-305-5124; F: 212-305-2741; sat2@columbia.edu).

#### CONFLICTS OF INTEREST

SSE is an inventor on patents covering the heparin-binding delivery system technology. Kuros Therapeutics has licensed these patents. SSE may receive royalties if additional licensing agreements occur as a result of this publication. Kuros did not fund this research and SSE does not have any role as a consultant or board member at Kuros. SWL, ST, and YX are inventors on a patent pending that covers the porous suture used in this study.

#### AUTHORS' CONTRIBUTION

SWL designed and executed the study with guidance from RHG, ST, HS, SSE, and YX. MLT produced the porous sutures with guidance from YX. SWL prepared the porous sutures for growth factor release testing and surgeries with assistance from SY, RJ, and MLT. SWL assessed growth factor release from sutures with assistance from SY and RJ. RHG and SY performed all surgeries with assistance from SWL and RJ. RJ and HS performed all sample preparation for histology, gene expression, and proteomics analyses. SWL wrote the manuscript, and RHG, ST, HS, SY, RJ, MLT, SSE, and YX provided edits.

#### SUPPORTING INFORMATION

Additional supporting information may be found in the online version of this article.

histological signs of angiogenesis and collagen deposition. There were no evident widespread biological effects throughout the tendon substance. There were significant differences in gene expression of the macrophage marker CD163 and anti-apoptotic factor BCL2L1; however, these differences were not corroborated by proteomics analysis. In summary, this study provided encouraging evidence of sustained delivery of biologically active CTGF from porous sutures without signs of a negative inflammatory reaction. With the development of a safe and effective method for generating a positive local biological response, future studies can explore additional methods for enhancing intrasynovial tendon repair.

## Keywords

porous suture; drug delivery; CTGF; connective tissue growth factor; flexor tendon

Although significant advances have been made in intrasynovial flexor tendon repair and rehabilitation over the past several decades, improvements have slowed while outcomes have remained highly variable and often unsatisfactory.<sup>1-5</sup> The paucicellular, hypovascular intrasynovial tendons of the hand have limited intrinsic healing capacity compared to extrasynovial tendons.<sup>6-8</sup> Adequate healing depends on cell migration, proliferation, and extracellular matrix protein synthesis at the repair site; however, these processes are inherently slow, particularly in the intrasynovial tendon environment. Intrasynovial flexor tendon repairs are therefore complicated frequently by adhesions between the tendon surface and the surrounding tendon sheath, repair-site gap formation, and repair-site failure, leading to impaired functional outcomes in injured digits.<sup>5,9</sup>

Recent efforts to address these problems have focused on biological approaches using growth factors and mesenchymal stem cells delivered on scaffolds either on the tendon surface,<sup>10-12</sup> interposed between the tendon stumps,<sup>13</sup> or within the repaired tendon.<sup>14-16</sup> While some encouraging results have demonstrated the therapeutic potential for cell- and growth factor-based approaches, large animal in vivo trials have not yet demonstrated consistent functional improvements.<sup>10-12,14-16</sup> In order to achieve meaningful clinical benefits amidst variable repair outcomes, approaches must induce substantial biological responses, but without deleterious side effects common among pleiotropic growth factors.<sup>16</sup> Furthermore, a biocompatible delivery system is required to positively impact the repairing tendon stumps, while avoiding negative inflammatory reactions that lead to the formation of adhesions, gap formation, and/or repair rupture.<sup>17</sup>

The current study aimed to address limitations of previous biological interventions for intrasynovial flexor tendon repair by combining CTGF, a growth factor recently shown to promote tendon regeneration in rodents,<sup>18-20</sup> with a novel porous suture delivery method.<sup>21</sup> Lee et al. recently demonstrated that CTGF embedded in a fibrin matrix can enrich tendon-resident CD146<sup>+</sup> stem/progenitor cells and promote neovascularization, tenogenic differentiation, collagen deposition, and matrix remodeling in a rat patellar tendon surgical model.<sup>18-20</sup> Porous sutures were recently developed as a method to deliver higher amounts of growth factor directly into the tendon mid-substance and repair interface, without requiring additional synthetic materials that have been shown to induce inflammatory

reactions.<sup>21</sup> Based on these prior results, we asked whether or not this porous suture delivery method could achieve sustained delivery of CTGF without negatively impacting repair mechanics or inducing inflammation, and furthermore we sought to determine if this approach could modulate the proliferative and remodeling responses after intrasynovial tendon injury and repair in a clinically relevant canine model.

## METHODS

### Preparation of Porous Sutures for Growth Factor Deliver

Surgical sutures with porous outer sheaths were created from pristine pseudo-monofilament surgical sutures (Supramid 4–0, HEA40, S. Jackson Inc., Alexandria, VA) by treating with a swelling and freeze-drying procedure, as described previously.<sup>21</sup> Before treatment, the commercially available, non-degradable sutures had a cable-type structure consisting of fine inner nylon-6,6 filaments enclosed by a nylon-6 sheath with a smooth surface. The sutures were soaked in a 500 mM CaCl<sub>2</sub> solution in methanol for 24 h at room temperature to induce swelling of the outer sheath and then quickly frozen in liquid nitrogen (–196°C). Then, samples were freeze-dried in a vacuum overnight to remove the methanol by sublimation, producing a highly porous structure.<sup>22,23</sup> Since all reagents used in this process were water soluble, their residues were readily removed by rinsing with water. This approach produced sutures with approximately 1 μm pores in the outer sheaths, but intact inner filaments (Fig. 1).<sup>21</sup>

### Biomechanics

Cadaver canine forepaw samples were obtained post-mortem from an unrelated study, stored at –20°C, and thawed at 4°C immediately before use. Flexor digitorum profundus (FDP) tendons were sharply transected in Zone II and repaired with unmodified or porous 4–0 Supramid core sutures using an 8-stranded Winters-Gelberman technique followed by a 5–0 proline running epitenon suture, as described previously ( $n = 10$  for porous sutures and  $n = 11$  for unmodified sutures).<sup>3,24</sup> RHG performed the ex vivo repairs with porous sutures and SY performed the ex vivo control repairs with unmodified sutures using the same technique. Following clinical-style repairs, cadaver FDP tendons were biomechanically evaluated as described previously.<sup>24–26</sup> After preconditioning, samples were pulled in uniaxial tension using a material testing machine (5866; Instron Corp., Norwood, MA) at 0.3 mm/s until failure and strain was tracked optically.<sup>24,26</sup> From the force-elongation curves, maximum load and load required to create a 2 mm gap in the repair (a clinically relevant measure of repair strength<sup>9</sup>) were determined. From the force-strain curves, rigidity (slope of the linear region), strain at 20 N force (approximating strains at physiologically relevant load levels<sup>27,28</sup>), and a modified version of resilience (area under the curve until yield) were determined.

### Growth Factor Loading and Sustained Release

Porous sutures, lyophilized after being washed with distilled water several times, were sterilized with poly(ethylene oxide) gas and loaded with recombinant human CTGF (BioVendor, Asheville, NC) in a heparin/fibrin delivery system (HBDS) for sustained release.<sup>14,29,30</sup> All pipette tips, tubes, and tools were either silanized or rinsed with TBS

containing 0.1% bovine serum albumin (BSA) prior to use to block inadvertent protein adsorption.

To coat with CTGF/HBDS, sterile sutures were first either cut into 15 mm pieces for in vitro release profile evaluation or left as 30 cm looped suture with a needle for in vivo surgical implantation. Sutures or suture segments were then submerged in TBS (pH 7.4) containing 0.1% w/v BSA (Sigma–Aldrich), 20 mg/ml human fibrinogen (plasminogen depleted, >95% clottable proteins; EMD Millipore), and CTGF/HBDS components at 4°C overnight to enable the components to permeate the porous suture and reach equilibrium at the desired CTGF/HBDS levels. The fibrinogen- and CTGF/HBDS-loaded sutures were then immersed in TBS containing 0.1% w/v BSA, 20 U/ml thrombin (Sigma–Aldrich), and 13.7 mM CaCl<sub>2</sub> for 2 h at 37°C to crosslink. Suture samples were washed by rinsing in TBS with 0.1% w/v BSA to remove unbound CTGF before collecting release profiles in vitro or implanting suture in vivo. The CTGF/HBDS components used for the two loading steps included: (i) a bi-domain HBDS peptide (sequence dLNQEQVSPK(βA)FAKLAARLYRKA-NH<sub>2</sub>, where dL denotes dansyl leucine, purity >95%; GenScript, Piscataway, NJ)<sup>14,30–33</sup>; (ii) heparin (Sigma–Aldrich H3393); and (iii) CTGF at a  $\left[4:1:\frac{1}{135}\right]$  stoichiometric molar ratio, calculated based on final CTGF concentrations (10, 20, 30, 40, 50, or 100 μg/ml for in vitro release studies,  $n = 2$  per group; 0 or 30 μg/ml for in vivo surgical studies). While there were small sample numbers at each loading concentration, several CTGF concentrations within a small range were evaluated to enhance reliability and enable identification of the optimal CTGF loading concentration for in vivo use.

After loading porous suture for in vitro release, 15 mm suture segments were incubated in 70 μl of TBS containing 0.1% w/v BSA at 37°C. All 70 μl of solution was collected at each time point and replaced with fresh TBS with 0.1% w/v BSA. The collected aliquots were placed in a silanized tube, centrifuged for 3 min at 16,100 *g*, and stored at –80°C before the amount of CTGF was quantified using an enzyme-linked immunosorbent assay (BioOcean, Shoreview, MN), performed following the manufacturer’s instructions, except using TBS with 0.1% w/v BSA for all dilution buffers to maintain a consistent buffer.

### Canine Flexor Tendon Injury and Repair Model

Ten 1- to 2- year-old female mongrel dogs (20–30 kg) were used in this study (Covance, Denver, PA), and all procedures were approved by the institutional Animal Studies Committee. Animal housing and welfare was provided by the institutional Division of Comparative Medicine. The effects of porous sutures loaded with or without CTGF were assessed in paired intrasynovial flexor tendon repairs in canines (Fig. 2), performed on two digits of one paw per animal ( $n = 10$  tendons per group). The FDP tendons of the medial and lateral right forepaw digits were sharply transected at the level of the proximal interphalangeal joint (within Zone II) and repaired using a porous core suture, loaded as described above with all HBDS components with or without CTGF at a 30 μg/ml soaking concentration (CTGF<sup>+</sup> group and CTGF<sup>–</sup> control group, respectively). All repairs were performed as described previously,<sup>10,14–16,32</sup> using an 8-stranded Winters-Gelberman core suture technique followed by a 5–0 nylon epitenon suture.<sup>3</sup> Controlled passive motion exercise was applied to the digits postoperatively to replicate the clinical scenario. The paws

were flexed fully and then extended to the limits of the extension block for 5 min daily, 6 days per week.<sup>34</sup>

The corresponding left digital flexor tendons served as normal controls (Normal group). All animals were euthanized 14 days after repair. Of the 10 repaired tendons within each repair group and normal controls, 6/10 were longitudinally transected into two parts consisting of approximately 2/3 and 1/3 of the tendon volume, within 5 mm on either side of the repair site. The smaller part was used for proteomics analysis, and the larger part was used for RNA isolation and subsequent gene expression analysis. The remaining tendons (4/10) were used for histological study and transmission electron microscopy. One tendon (CTGF<sup>-</sup> group, histological sample) formed a gap greater than 3 mm and was therefore excluded along with the paired tendon from the same animal (CTGF<sup>+</sup> group).

## Histology and Transmission Electron Microscopy

**Histological Section Preparation**—For morphological assessment, a 20 mm tendon fragment was obtained from each repaired tendon, with the transection site in the middle. The tendon fragments were trimmed at both ends to generate a center piece (10 mm in length) and two end pieces (5 mm in length). The center pieces and end pieces were used for histology and transmission electron microscopy (TEM), respectively. The histological samples were fixed in 4% paraformaldehyde overnight. After washing and dehydrating, the histology samples were embedded in paraffin and serial coronal paraffin sections (5 μm thick) were prepared.<sup>10,12</sup> Hematoxylin and eosin (H&E), Russell-Movat pentachrome (American MasterTech, Lodi, CA), or reticular staining were performed. Reticular staining was chosen to assess vascular ingrowth since it is a well characterized stain, and there are no validated CD34 antibodies available for the canine. Immunohistochemical staining for CD146 and Ki67 was also performed to label for tendon-resident CD146<sup>+</sup> stem/progenitor cells and proliferating cells, respectively.

**Cell Counting Protocol**—Histological slides from the middle of the flexor tendon thickness, prepared with H&E staining, were used to assess cell counts near the suture surface ( $n = 3$  tendons per group, paired by animal). Digital slides were analyzed blindly using a custom MATLAB script that manually identified the tendon laceration interface, then divided each side into thirds (approximately 3 mm long each) for cell counting. The script automatically identified the suture sections by thresholding the grayscale image, with user oversight. This enabled accurate calculation of the area of the tissue section within 70 μm of the suture surface, which was used to create output images for cell counting and also used for normalization. Cells in each section were counted manually in ImageJ and normalized by tissue area. Normalized cell counts from corresponding segments on each side of a slide were averaged as a single experimental sample.

**Transmission Electron Microscopy (TEM)**—Ultrathin cross sections (90–100 nm) of flexor tendon were prepared from the TEM samples. Cross sections were taken from the TEM tendon sample end closest to the transection site to ensure that the samples included suture material. TEM images were taken at 2,500× and displayed at approximately 1,250× magnification. Collagen fibrils were automatically identified by thresholding the image with

a custom MATLAB script, and fibril diameter and distance from the 10 closest neighboring fibrils (a measure of fibril density) were calculated.

### Gene Expression

Total RNA isolation, cDNA synthesis, and gene expression assays were performed as described previously.<sup>10,12,35</sup> The gene expression profile in repaired tendons 14 days after repair was determined using TaqMan® real-time PCR (Applied Biosystems, Woolston, UK) by the Washington University Genome Technology Access Center using the Biomark™ HD system (Fluidigm, San Francisco, CA). The relative abundance of target genes in repaired digits was analyzed with the comparative Ct ( $2^{-Ct}$ ) method using *GAPDH* and *PP1B* as endogenous reference genes. All gene expression results are shown as fold changes compared to the average gene expression levels in contra-lateral non-operated, normal digits (2nd and 5th) from the same animal. All TaqMan primers and probes used in this study were obtained from Applied Biosystems (Foster City, CA).

### Proteomics

Protein sample preparation and quantitative proteomics analysis were performed by the Proteomics Core Laboratory at Washington University using a tandem-mass-tag-based assay, as described previously.<sup>12</sup> The PROC MIXED models (SAS Institute, Cary, NC) were applied to proteomics data to identify proteins differentially expressed between three different conditions (Normal, CTGF<sup>-</sup>, CTGF<sup>+</sup>). Protein functional classification was performed on selected proteins using the UniProt Knowledgebase (UniProtKB) at UniProt (<http://www.uniprot.org>).

### Statistics

All data are shown as box plots, with the median and range (minimum, 25th percentile, 75th percentile, and maximum), unless otherwise noted. For ex vivo cadaver flexor tendon biomechanics data, unpaired two-tailed Student's *t*-tests were used to compare unmodified and porous suture groups. For cell counts, a 2-way analysis of variance (ANOVA) was performed to compare normalized cell counts grouped by CTGF delivery and position, followed by Fisher's least significant difference post hoc tests. For collagen fibril size comparisons, three representative TEM images per group were combined and fibril diameters were compared with an unpaired Wilcoxon rank-sum test. For gene expression, paired Wilcoxon signed-rank tests were used to compare the fold change compared to normal for CTGF<sup>-</sup> and CTGF<sup>+</sup> groups. Changes that yielded  $0.05 < p < 0.1$  are marked as nonsignificant (N.S.). For proteomics data, an ANOVA was used to compare relative protein abundance between groups. The obtained *p*-values were further corrected using Benjamini-Hochberg's method.

## RESULTS

### Ex vivo Biomechanics

We previously confirmed non-inferiority of the porous sutures compared to unmodified sutures in single-strand tests.<sup>21</sup> In the current study, porous sutures were evaluated using clinical-style cadaver flexor tendon repairs (Fig. 3A). For each measured mechanical

property, the 95% confidence intervals for difference between the means and the percentage change between groups are listed in Table S1. The loads creating a 2 mm gap, failure loads, repair rigidities, repair resiliencies, and strains created by a physiologically relevant 20 N load are displayed for each group in Figure 3B–E, and G, respectively. Load versus strain curves for all samples are shown in Figure 3F. The maximum load and resilience of repairs were comparable between groups, indicating porous sutures were appropriate for in vivo use. There was a statistically significant 22% decrease in load to create a 2 mm gap using porous sutures; however, the decrease was not clinically meaningful since repairs remained substantially stronger than functional requirements for controlled rehabilitation and normal grasp strength (approximately 35 N).<sup>36</sup> Similarly, the 25% decrease in rigidity and 17% increase in strain created by a 20 N load were statistically but not clinically significant.

Surgical handling was notably different between the unmodified sutures and the uncoated porous sutures in cadaver tendon. While the unmodified sutures have a smooth surface that enabled low-friction suture passage, porous sutures had substantially higher surface area that increased friction during suture passage. That difference was likely exacerbated by using cadaver instead of living tissue. The high porous suture friction was ameliorated by adding PBS onto the suture before passage. It was expected that coating the porous sutures with CTGF/HBDS would fill the pores with fibrin hydrogel, reduce the effective surface area, and further decrease friction. Indeed, the friction experienced by the surgeon when passing sutures through tendon was qualitatively lower during in vivo experiments using porous sutures coated with CTGF/HBDS than it was during ex vivo experiments with uncoated porous sutures.

### Ex vivo CTGF Loading and Release

A major objective of this study was to attain sufficient biofactor loading capacity on suture to drive a biological effect. To evaluate the potential for sustained release of growth factor, porous sutures were loaded with various concentrations of CTGF in HBDS (10, 20, 30, 40, 50, and 100 µg/ml CTGF soaking concentration). Sutures demonstrated sustained release of CTGF over at least 14 days in vitro (Fig. 4). Loading capacity was partially limited by CTGF and HBDS component precipitation when higher concentrations were used during loading (Table 1). Therefore, while the CTGF loaded into the soaking buffer progressively increased with each subsequent concentration, the effective concentration decreased when visible precipitate formed above ≈30 µg/ml CTGF (Table 1). The maximum CTGF release was observed from porous suture segments loaded with 30–50 µg/ml CTGF/HBDS loading solution, where precipitate formation was limited but the loading concentration was still high. All samples in the 30–50 µg/ml CTGF loading concentration range yielded consistent release profiles. Therefore, 30 µg/ml was selected for in vivo experiments to minimize any unintended effects from precipitate formation. Porous sutures loaded in 30 µg/ml CTGF/HBDS demonstrated burst release of 0.50–1.50 (ng CTGF)/(cm suture)/day for the first few days, followed by sustained release of approximately 0.15 (ng CTGF)/(cm suture)/day through day 14. Since approximately 70 mm of suture is delivered within 3 mm of the repair site in the traversing strands and the terminal knot, this release level corresponded to concentrations of 60–150 ng/ml daily burst delivery and 10–20 ng/ml daily sustained release from suture within 3 mm of the tendon laceration site.

## In vivo Biological Effects of CTGF-Laden Porous Sutures

FDP tendon transections and repairs were performed with porous sutures loaded with 0 or 30  $\mu\text{g/ml}$  CTGF. CTGF delivery within the repaired flexor tendon was achieved without adhesion or repair-site gap formation upon dissection at 14 days in the CTGF<sup>+</sup> group. In one of the 20 repaired tendons, a >3.0 mm gap was noted (CTGF<sup>-</sup> group, histological sample), and was therefore excluded along with the paired tendon. There were no macroscopic indicators of inflammation or other deleterious effects at 14 days, such as wound dehiscence, pus formation, swelling in the digit and tendon sheath, blood within the sheath, or redness on the volar tendon surface. There were no or only very mild adhesions. This result positively contrasts with our historical experience, where canine flexor tendon repairs are highly sensitive to inflammatory stimuli.<sup>15,37</sup>

Histological assessment with H&E demonstrated high quality repairs with little difference between groups at low magnification (Fig. 5, top). However, normalized cell counts under higher magnification demonstrated increased cellularity immediately surrounding the suture tracks (within 70  $\mu\text{m}$ , Fig. 5C–F, quantified in Fig. 5G,  $p = 0.022$  for CTGF effects and  $p = 0.003$  for position effects,  $n = 3$  per group), especially at the repair interface. There were also higher cell counts far from the repair interface in each of the three CTGF<sup>+</sup> samples than their paired CTGF<sup>-</sup> controls, though the variability precluded post hoc significance (Fig. 5G). Pentachrome stains<sup>38,39</sup> demonstrated increased staining for new collagen (yellow) instead of mature collagen (red) in CTGF<sup>+</sup> samples than CTGF<sup>-</sup> controls, both at a macroscopic level and near the suture surface (Fig. 6A–D). Reticular staining indicated likely angiogenesis surrounding CTGF<sup>+</sup> sutures far from the repair interface (Fig. 6H). While CD146 staining did not show apparent differences between groups (Fig. S1), we note that it is challenging to see differences with this staining method since TSPCs are rare in vivo, and <1% of isolated tendon cells stain for CD146.<sup>19</sup> Many, but not all, cells near CTGF<sup>+</sup> suture surfaces stained for Ki67, while few cells stained for Ki67 near CTGF<sup>-</sup> suture surfaces (Fig. S2). This Ki67 staining pattern indicates that the increased cellularity near the CTGF<sup>+</sup> suture surface was likely due to a combination of increased cell migration and cell proliferation.

TEM images showed cell activity immediately adjacent to the CTGF<sup>+</sup> suture, with a clear layer of glycoproteins surrounding the CTGF<sup>-</sup> suture (Fig. 7A and C) but not the CTGF<sup>+</sup> suture (Fig. 7B and D). Collagen fibrils adjacent to the CTGF<sup>+</sup> suture were 33% smaller and 23% closer to their nearest 10 neighboring fibrils than fibrils near CTGF<sup>-</sup> suture, on average ( $p < 0.001$  for both measures). The smaller, more densely packed collagen fibrils near CTGF<sup>+</sup> suture are indicative of newly synthesized collagen or a different collagen subtype compared to CTGF<sup>-</sup> control repairs (Fig. 7E). CTGF-laden sutures also had some sites where collagen appeared to be penetrating the porous suture surface (Fig. 7D, arrows).

Gene expression did not demonstrate large differences between CTGF<sup>+</sup> sutures and CTGF<sup>-</sup> control porous sutures, each normalized to contralateral non-operated tendons (Fig. 8). There were 64% (N.S.), 52%, and 52% (N.S.) increases in the expression fold change of the monocyte/macrophage M2 marker *CD163*, the anti-inflammatory cytokine *IL10*, and the anti-apoptotic factor *BCL2L1*, respectively, due to CTGF. There were 24 and 19% (N.S.) decreases in the expression fold change of collagen 2 and *IL6*, respectively. However, despite this anti-inflammatory and anti-apoptotic gene expression increase, expression levels



of collagen 1 and 3 and tenogenic markers scleraxis and tenomodulin were similar between groups. There were no significant differences in the expression of the matrix metalloproteinase *MMP9* or the cytokine related genes *IL1-RN* or *IL4*.

Proteomics analysis identified 512 proteins from normal and suture repaired flexor tendons. Compared to normal tendons, the relative abundances of 129 proteins were modified after tendon injury and suture repair in the presence or absence of CTGF, while no apparent differences in protein abundances were detected between the two suture treatments. Consistently, principal component analysis separated normal tendons from sutured tendons, but did not separate treatment groups with and without CTGF according to the first three principal components (Fig. 9). Further characterization of the 129 modified proteins using the Panther Classification System revealed the function of 108 proteins (supplemental Table S1). Only a small percentage of proteins were engaged in biological adhesion (2.5%) and immune system processes (4.9%) that potentially impact tendon healing. There were no differences in inflammatory protein levels (e.g., *NCF2*, *PTGR1*, and *SOD3*) between the tendons repaired with CTGF<sup>+</sup> or CTGF<sup>-</sup> porous sutures and historical repair-only controls with unmodified suture.<sup>12</sup>

## DISCUSSION

The goal of this study was to achieve biological augmentation of intrasynovial flexor tendon healing via sustained suture-based delivery of an active growth factor without adverse effects such as adhesion formation or deleterious inflammation. To accomplish these objectives, we impregnated and coated porous sutures<sup>21</sup> with a sustained delivery system<sup>33,40</sup> to deliver CTGF, a growth factor with promising results for tendon regeneration.<sup>18–20</sup> Sutures have several attractive properties for growth factor delivery in tendon repair. First, they are commonly used in conventional repairs and therefore do not require additional material that could damage tissue or cause inflammation. Second, the suture strands and knot reside within the tendon midsubstance and the repair interface, where growth factors may directly stimulate cell migration, differentiation, and matrix synthesis. Third, neovascularization and cell infiltration within tendon has been shown to occur along suture tracks,<sup>41</sup> so growth factor delivery along these tracks may accelerate and guide these processes. Over the last two decades, several experiments have evaluated growth factor delivery on sutures for intrasynovial flexor tendon,<sup>42</sup> Achilles tendon,<sup>43,44</sup> and rotator cuff tendon<sup>45</sup> repair, with mixed preliminary success. None of these approaches have progressed to clinical use. Prior approaches have focused on coating the surface of a solid suture with growth factors. Solid suture, however, has limited surface area and exposes the growth factor directly to the surrounding tissue. As a result, bolus release of growth factor typically occurs within a few hours to days following application.<sup>45–48</sup> Furthermore, the growth factor dose is markedly limited since the thin coatings contain very low volumes. In addition, thin surface films are often weakly bound, so growth factor are easily stripped off of the suture during implantation.<sup>21</sup> Despite these challenges, suture remains a promising delivery approach, provided that methods can be developed for the administration of increased dosages over sustained time-courses following repair.

Recently, we established a method for modifying nylon sutures to create porous outer sheaths, thereby increasing growth factor loading capacity and facilitating sustained release.<sup>21</sup> In the current study, the porous sutures loaded with CTGF in a fibrin matrix with a heparin-based delivery system exhibited a burst of CTGF followed by sustained release over 14 days in vitro (Fig. 4) at a dosage of approximately 10–20 ng/ml tendon volume, which is at the lower end of the effective range used in vitro.<sup>18</sup> Furthermore, nylon sutures, modified with porous outer sheaths, retained sufficient mechanical properties for surgical use, as demonstrated by non-inferiority compared to commercially available sutures in biomechanical assessments of single suture strands.<sup>21</sup> The mechanical properties of clinical-style repairs using porous sutures were reduced by some measures but still within 25% of controls (Fig. 3). This difference is partially attributable to surgeon-to-surgeon variability, given that the mechanical properties of porous suture repairs were non-inferior to historical controls.<sup>24,26</sup> The modestly altered mechanical properties were sufficiently close to controls and non-inferior to historical data to assuage concerns over surgical implementation.<sup>24,26</sup> The time zero biomechanics results described here are sufficient to withstand passive range of motion and normal hand function (approximately 35 N)<sup>36</sup> throughout the healing process. Importantly, only one tendon out of 20 had gapping (5%, in the CTGF<sup>-</sup> group), despite our previous experience of ~15% rupture rates in this model (and clinically) when using regular sutures.<sup>12,15</sup>

The promising ex vivo mechanical and biological characteristics of the porous sutures encouraged us to assess their efficacy in a clinically relevant in vivo canine flexor tendon repair model. The porous sutures, with and without growth factor, did not elicit an inflammatory response at 14 days following surgical repair based on histological, gene expression, and proteomics evaluations. Based on historical experience with this animal model, proteomics has been particularly sensitive for identifying inflammatory effects.<sup>10,12,15</sup> The lack of significant differences in inflammatory protein markers between porous suture groups with and without CTGF and historical controls using unmodified suture indicates that this porous suture delivery approach is non-inflammatory and not deleterious to the repair. This safe, targeted, sustained delivery approach represents a significant improvement compared to previous growth factor delivery strategies for tendon repair.<sup>11,15,17</sup>

Histological assessment provided encouraging indications of local biological effects around the suture surface in the CTGF<sup>+</sup> group. Cell numbers increased at the repair interface and along the suture track of CTGF-laden sutures, indicating increased local cell migration and/or proliferation (Fig. 5, Fig. S2). The most pronounced cellular effect along the suture strand-tendon interface was in regions distant from the repair site. This pattern was expected based on typical neovascularization patterns following intra-synovial flexor tendon repair: since the canine lacks a vinculum longum and the repair was performed in the middle of a 3 cm avascular zone, neovascular ingrowth occurs progressively from the proximal, and distal stumps toward the repair interface.<sup>41</sup> Furthermore, CTGF was delivered along the entire length of the suture, so we expect effects both at the repair site where the suture knot is buried and along suture distant from the repair interface. Pentachrome and reticular stains also indicated increased collagen production and angiogenesis in areas adjacent to the CTGF-laden porous sutures compared to porous sutures without CTGF (Fig. 6). Light and

transmission electron microscopic sections provided evidence of cellular alignment along the suture surface and possible tissue ingrowth into the porous suture structure (Figs. 5–7). Tissue ingrowth into porous structures for abdominal hernia repair<sup>49,50</sup> and bone implants<sup>51–54</sup> has been shown to strengthen the repair. Similarly, tissue ingrowth into suture would have a strengthening effect on tendon repair by facilitating load transfer between suture and the surrounding tissue along the suture length. A similar mechanical principle has been previously described for improved repairs using adhesive coatings on sutures.<sup>24</sup>

There are several limitations to the current study. It is possible that the CTGF dosage we employed was insufficient to induce a substantial effect throughout the healing tendon. We performed a dose-response study and selected the loading concentration that led to the greatest in vitro CTGF release. Despite dose maximization, in vitro CTGF release was at the lower end of a biologically effective range in culture. Potential opportunities for increasing CTGF effects include increasing the suture pore size in order to create greater capacity within the suture sheath, developing an alternative sustained release system to achieve higher loading yield, or utilizing a modified version of CTGF. Effective CTGF levels are determined not only by flux into the tendon, but also by clearance out of the tissue (half-life) and by potency of the released growth factor. Similarly, protein engineering approaches to modify the binding site may generate a CTGF protein drug with higher binding affinity to the cell surface receptor and more potent effect. The delivery approach could be revisited using an alternative growth factor, though side effects from pleiotropic growth factors require careful monitoring. Finally, this study evaluated effects at a time point within the proliferative stage of repair. The biological effects seen locally around the suture may induce a larger effect over time as those cells continue to proliferate and produce matrix. While 14 days may be too short for functional outcome measurement in this clinically relevant model, it does provide data that encourages functional biomechanical assessment at later time-points.

Cell- and growth factor-based approaches have the potential to guide the healing response and to overcome the limitations of mechanical suture repair. This study, which demonstrates the first in vivo use of a new approach to deliver biologically active factors into the repair site, successfully mitigated the inflammatory concerns that were noted with prior biofactor delivery approaches.<sup>14–16</sup> While only localized biological effects were seen in our experiment, the findings noted here are encouraging and warrant future investigation to increase biofactor delivery from suture with porous outer sheaths.

## Supplementary Material

Refer to Web version on PubMed Central for supplementary material.

## Acknowledgments

Grant sponsor: National Institute of Arthritis and Musculoskeletal and Skin Diseases; Grant numbers: F30-AR069491, P30-AR057235, R01-AR062947.

We appreciate Ms. Zifei Sun's support modifying nylon sutures to create porous outer sheaths. The Washington University Musculoskeletal Histology and Morphometry Core, Molecular Microbiology Imaging Facility, Genome Technology Access Center, and Proteomics Core Laboratory assisted with assessing outcomes following surgical

repair. This work was supported by National Institutes of Health grants R01-AR062947 (to RHG, ST, and SSE), F30-AR069491 (to SWL), and a Washington University Musculoskeletal Research Center Translational Research Award (NIH P30-AR057235).

## References

1. Potenza AD. Tendon healing within the flexor digital sheath in the dog. *J Bone Jt Surg Am.* 1962; 44-A:49–64.
2. Kessler I, Nissim F. Primary repair without immobilization of flexor tendon division within the digital sheath. An experimental and clinical study. *Acta Orthop Scand.* 1969; 40:587–601. [PubMed: 4907784]
3. Winters SC, Gelberman RH, Woo SL, et al. The effects of multiple-Strand suture methods on the strength and excursion of repaired intrasynovial flexor tendons: a biomechanical study in dogs. *J Hand Surg Am.* 1998; 23:97–104. [PubMed: 9523962]
4. Boyer MI, Strickland JW, Engles DR, et al. Flexor Tendon Repair and Rehabilitation: state of the art in 2002. *Instr Course Lect.* 2003; 52:137–161. [PubMed: 12690845]
5. Woo SL-Y, Gelberman RH, Cobb NG, et al. The importance of controlled passive mobilization on flexor tendon healing. *Acta Orthop Scand.* 1981; 52:615–622. [PubMed: 7331798]
6. Gelberman RH, Vandeberg JS, Lundborg GN, et al. Flexor tendon healing and restoration of the gliding surface. An ultrastructural study in dogs. *J Bone Joint Surg Am.* 1983; 65:70–80. [PubMed: 6848538]
7. Fenwick SA, Hazleman BL, Riley GP. The vasculature and its role in the damaged and healing tendon. *Arthritis Res.* 2002; 4:252–260. [PubMed: 12106496]
8. Abrahamsson SO, Gelberman RH, Lohmander SL. Variations in cellular proliferation and matrix synthesis in intrasynovial and extrasynovial tendons: an in vitro study in dogs. *J Hand Surg Am.* 1994; 19:259–265. [PubMed: 8201191]
9. Gelberman RH, Boyer MI, Brodt MD, et al. The effect of gap formation at the repair site on the strength and excursion of intrasynovial flexor tendons. *J Bone Jt Surg Am.* 1999; 81-A:975–982.
10. Shen H, Korpakakis I, Havlioglu N, et al. The effect of mesenchymal stromal cell sheets on the inflammatory stage of flexor tendon healing. *Stem Cell Res Ther.* 2016; 7:144. [PubMed: 27677963]
11. Zhao C, Ozasa Y, Shimura H, et al. Effects of lubricant and autologous bone marrow stromal cell augmentation on immobilized flexor tendon repairs. *J Orthop Res.* 2016; 34:154–160. [PubMed: 26177854]
12. Gelberman RH, Linderman SW, Jayaram R, et al. Combined administration of ASCs and BMP-12 promotes an M2 macrophage phenotype and enhances tendon healing. *Clin Orthop Relat Res.* 2017; 475:2318–2331. [PubMed: 28462460]
13. Spalazzi JP, Dagher E, Doty SB, et al. In vivo evaluation of a multiphased scaffold designed for orthopaedic interface tissue engineering and soft tissue-to-bone integration. *J Biomed Mater Res—Part A.* 2008; 86:1–12.
14. Manning CN, Schwartz AG, Liu W, et al. Controlled delivery of mesenchymal stem cells and growth factors using a nanofiber scaffold for tendon repair. *Acta Biomater.* 2013; 9:6905–6914. [PubMed: 23416576]
15. Gelberman RH, Shen H, Korpakakis I, et al. Effect of adipose-derived stromal cells and BMP12 on intrasynovial tendon repair: a biomechanical, biochemical, and proteomics study. *J Orthop Res.* 2016; 34:630–640. [PubMed: 26445383]
16. Thomopoulos S, Kim HM, Das R, et al. The effects of exogenous basic fibroblast growth factor on intrasynovial flexor tendon healing in a canine model. *J Bone Joint Surg Am.* 2010; 92A:2285–2293.
17. Linderman SW, Gelberman RH, Thomopoulos S, et al. Cell and biologic-based treatment of flexor tendon injuries. *Oper Tech Orthop.* 2016; 26:206–215. [PubMed: 28042226]
18. Lee CH, Shah B, Moioli EK, et al. CTGF directs fibroblast differentiation from human mesenchymal stem/stromal cells and defines connective tissue healing in a rodent injury model. *J Clin Invest.* 2010; 120:3340–3349. [PubMed: 20679726]

19. Lee CH, Lee FY, Tarafder S, et al. Harnessing endogenous stem/progenitor cells for tendon regeneration. *J Clin Invest*. 2015; 125:2690–2701. [PubMed: 26053662]
20. Tarafder S, Chen E, Jun Y, et al. Tendon stem/progenitor cells regulate inflammation in tendon healing via JNK and STAT3 signaling. *FASEB J*. 2017; 31:3991–3998. [PubMed: 28533328]
21. Li J, Linderman SW, Zhu C, et al. Surgical sutures with porous sheaths for the sustained release of growth factors. *Adv Mater*. 2016; 28:4620–4624. [PubMed: 27059654]
22. Samitsu S, Zhang R, Peng X, et al. Flash freezing route to mesoporous polymer nanofibre networks. *Nat Commun*. 2013; 4:2653. [PubMed: 24145702]
23. Im SH, Jeong U, Xia Y. Polymer hollow particles with controllable holes in their surfaces. *Nat Mater*. 2005; 4:671–675. [PubMed: 16086022]
24. Linderman SW, Korpakakis I, Gelberman RH, et al. Shear lag sutures: improved suture repair through the use of adhesives. *Acta Biomater*. 2015; 23:229–239. [PubMed: 26022966]
25. Thomopoulos S, Kim HM, Silva MJ, et al. Effect of bone morphogenetic protein 2 on tendon-to-bone healing in a canine flexor tendon model. *J Orthop Res*. 2012; 30:1702–1709. [PubMed: 22618762]
26. Korpakakis I, Linderman SW, Thomopoulos S, et al. Enhanced zone II flexor tendon repair through a new half hitch loop suture configuration. *PLoS ONE*. 2016; 11:e0153822. [PubMed: 27101409]
27. Lieber RL, Amiel D, Kaufman KR, et al. Relationship between joint motion and flexor tendon force in the canine forelimb. *J Hand Surg Am*. 1996; 21:957–962. [PubMed: 8969415]
28. Lieber RL, Silva MJ, Amiel D, et al. Wrist and digital joint motion produce unique flexor tendon force and excursion in the canine forelimb. *J Biomech*. 1999; 32:175–181. [PubMed: 10052923]
29. Sakiyama-Elbert SE, Hubbell JA. Controlled release of nerve growth factor from a heparin-containing brin-based cell ingrowth matrix. *J Control Release*. 2000; 69:149–158. [PubMed: 11018553]
30. Sakiyama-Elbert SE, Das R, Gelberman RH, et al. Controlled-release kinetics and biologic activity of platelet-derived growth factor-BB for use in flexor tendon repair. *J Hand Surg Am*. 2008; 33A:1548–1557.
31. Gelberman RH, Thomopoulos S, Sakiyamaelbert SE, et al. The early effects of sustained platelet-derived functional and structural properties of repaired intrasynovial flexor tendons: an in vivo biomechanic study at 3 weeks in canines. *J Hand Surg Am*. 2007; 32A:373–379.
32. Thomopoulos S, Das R, Silva MJ, et al. Enhanced flexor tendon healing through controlled delivery of PDGF-BB. *J Orthop Res*. 2009; 27:1209–1215. [PubMed: 19322789]
33. Sakiyama-Elbert SE, Hubbell JA. Development of fibrin derivatives for controlled release of heparin-binding growth factors. *J Control Release*. 2000; 65:389–402. [PubMed: 10699297]
34. Gelberman RH, Amiel D, Gonsalves M, et al. The influence of protected passive mobilization on the healing of flexor tendons: a biochemical and microangiographic study. *Hand*. 1981; 13:120–128. [PubMed: 7286796]
35. Shen H, Gelberman RH, Silva MJ, et al. BMP12 induces tenogenic differentiation of adipose-derived stromal cells. *PLoS ONE*. 2013; 8:e77613. [PubMed: 24155967]
36. Schuind F, Garcia-Elias M, Cooney WP, et al. Flexor tendon forces: in vivo measurements. *J Hand Surg Am*. 1992; 17:291–298. [PubMed: 1564277]
37. Manning CN, Havlioglu N, Knutsen E, et al. The early inflammatory response after flexor tendon healing: a gene expression and histological analysis. *J Orthop Res*. 2014; 32:645–652. [PubMed: 24464937]
38. Burssens P, Forsyth R, Steyaert A, et al. Influence of burst TENS stimulation on collagen formation after Achilles tendon suture in man. A histological evaluation with Movat's pentachrome stain. *Acta Orthop Belg*. 2005; 71:342–346. [PubMed: 16035709]
39. Movat HZ. Demonstration of all connective tissue elements in a single section; pentachrome stains. *AMA Arch Pathol*. 1955; 60:289–295. [PubMed: 13248341]
40. Thomopoulos S, Das R, Sakiyama-Elbert S, et al. BFGF and PDGF-BB for tendon repair: controlled release and biologic activity by tendon fibroblasts in vitro. *Ann Biomed Eng*. 2010; 38:225–234. [PubMed: 19937274]

41. Gelberman RH, Khabie V, Cahill CJ. The revascularization of healing flexor tendons in the digital sheath. *J Bone Joint Surg.* 1991; 73:868–881. [PubMed: 1712787]
42. Hamada Y, Katoh S, Hibino N, et al. Effects of monofilament nylon coated with basic fibroblast growth factor on endogenous intrasynovial flexor tendon healing. *J Hand Surg Am.* 2006; 31:530–540. [PubMed: 16632043]
43. Chamberlain CS, Lee J-S, Leiferman EM, et al. Effects of BMP-12-releasing sutures on achilles tendon healing. *Tissue Eng Part A.* 2015; 21:916–927. [PubMed: 25354567]
44. Rickert M, Jung M, Adiyaman M, et al. A growth and differentiation factor-5 (GDF-5)-coated suture stimulates tendon healing in an Achilles tendon model in rats. *Growth Factors.* 2001; 19:115–126. [PubMed: 11769971]
45. Uggen C, Dines J, McGarry M, et al. The effect of recombinant human platelet-derived growth factor BB-coated sutures on rotator cuff healing in a sheep model. *Arthrosc—J Arthrosc Relat Surg.* 2010; 26:1456–1462.
46. Obermeier A, Schneider J, Wehner S, et al. Novel high efficient coatings for anti-microbial surgical sutures using chlorhexidine in fatty acid slow-release carrier systems. *PLoS ONE.* 2014; 9:e101426. [PubMed: 24983633]
47. Fuchs TF, Surke C, Stange R, et al. Local delivery of growth factors using coated suture material. *Sci World J.* 2012; 2012:1–8.
48. Younesi M, Donmez BO, Islam A, et al. Heparinized collagen sutures for sustained delivery of PDGF-BB: delivery profile and effects on tendon-derived cells in vitro. *Acta Biomater.* 2016; 41:100–109. [PubMed: 27240725]
49. Bachman S, Ramaswamy A, Ramshaw B. *Hernia repair sequelae.* Berlin, Heidelberg: Springer; 2010. Tissue ingrowth, adhesion, and mesh contraction; 345–352.
50. Bauer JJ, Harris MT, Kreel I, et al. Twelve-year experience with expanded polytetrafluoroethylene in the repair of abdominal wall defects. *Mt Sinai J Med.* 1999; 66:20–25. [PubMed: 9989101]
51. Issack PS. Use of porous tantalum for acetabular reconstruction in revision hip arthroplasty. *J Bone Jt Surg Am.* 2013; 95:1981–1987.
52. Bobyn JD, Pilliar RM, Cameron HU, et al. Osteogenic phenomena across endosteal bone-implant spaces with porous surfaced intramedullary implants. *Acta Orthop Scand.* 1981; 52:145–153. [PubMed: 7246092]
53. Hacking SA, Bobyn JD, Toh KK, et al. Fibrous tissue ingrowth and attachment to porous tantalum. *J Biomed Mater Res.* 2000; 52:631–638. [PubMed: 11033545]
54. Bobyn JD, Stackpool GJ, Hacking SA, et al. Characteristics of bone ingrowth and interface mechanics of a new porous tantalum biomaterial. *J Bone Jt Surg Br.* 1999; 81:907–914.

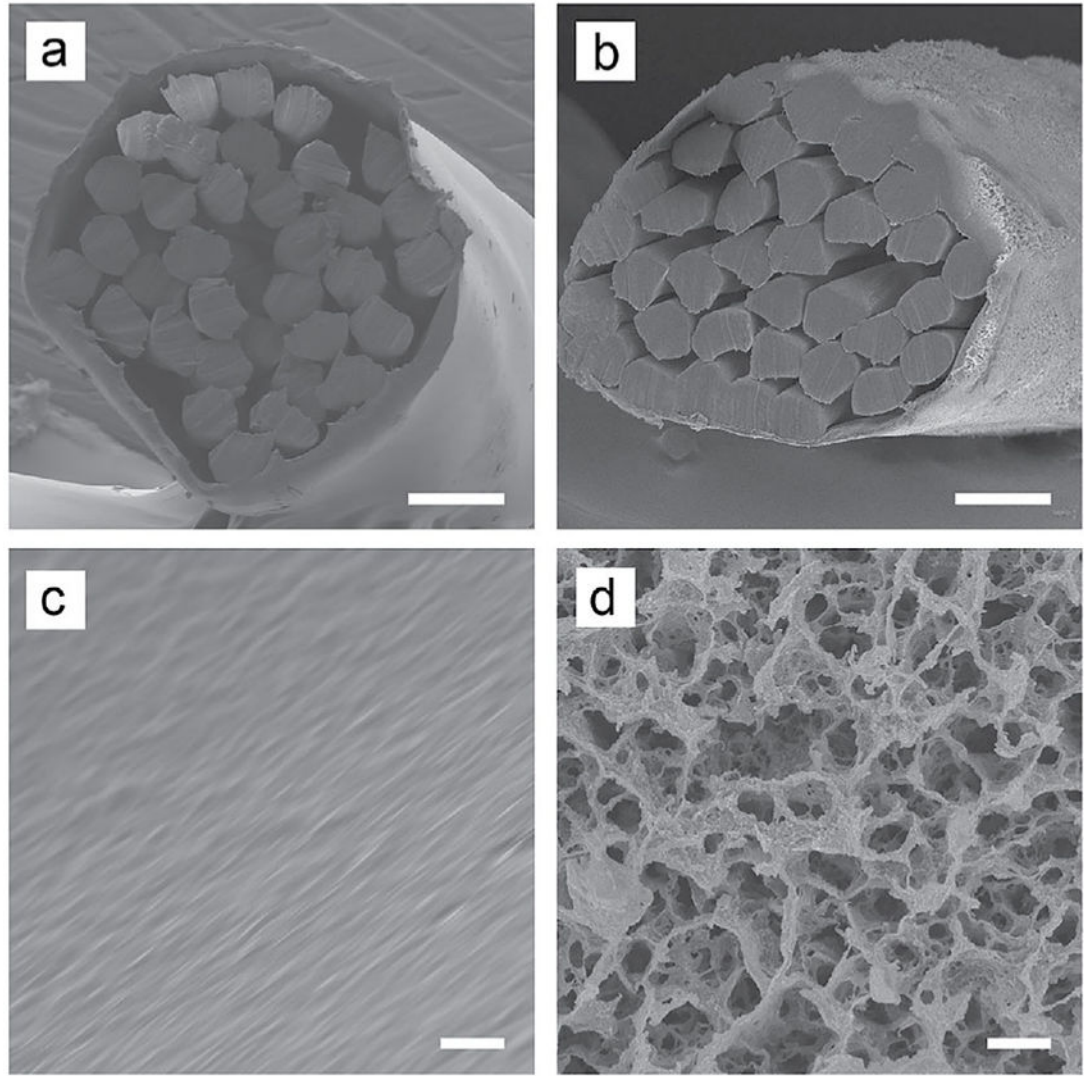


**Figure 1.** SEM images of the (A,B) cross sections and (C,D) side surfaces of unmodified (A,C) and porous (B,D) sutures. Scale bars: 50  $\mu\text{m}$  in panels (A,B) and 2  $\mu\text{m}$  in panels (C,D). Figure reproduced with permission from Li et al.<sup>21</sup>

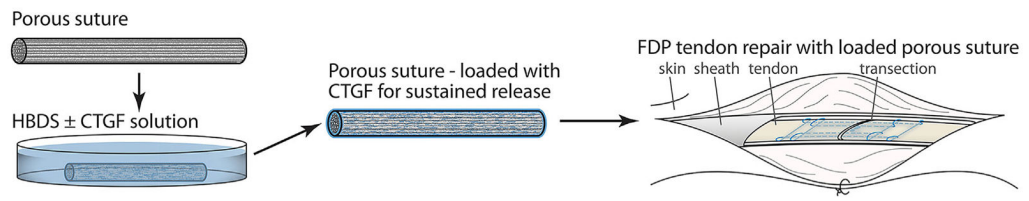


**Figure 2.**

Porous sutures with high surface area and loading capacity were used to deliver CTGF in a sustained fashion directly to the injury site within an FDP tendon repair.



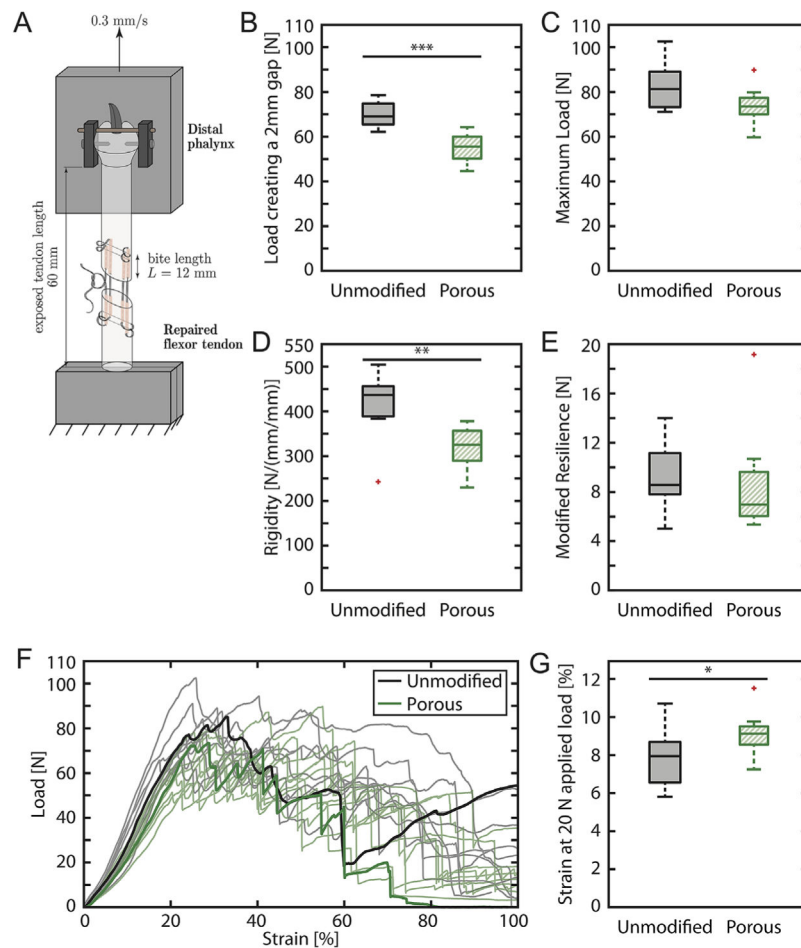


**Figure 3.** Tensile mechanical testing of the unmodified sutures (black) and porous sutures (green) in an 8-stranded Winters-Gelberman flexor digitorum profundus tendon repair: (A) mechanical testing schematic, (B) load to create a 2 mm gap, (C) maximum load, (D) rigidity, (E) modified resilience, (F) load versus strain curves for all samples, with representative curves bolded, and (G) strain at 20 N applied load.  $N = 11$  for the unmodified suture group and  $n = 10$  for the porous suture group. Overbars and asterisks denote statistically significant differences (\* $p < 0.05$ , \*\* $p < 0.01$ , \*\*\* $p < 0.001$ ,  $n = 10-11$ ). Mechanical properties of repairs with porous sutures were modestly decreased and similar to historical control data.<sup>24,26</sup>

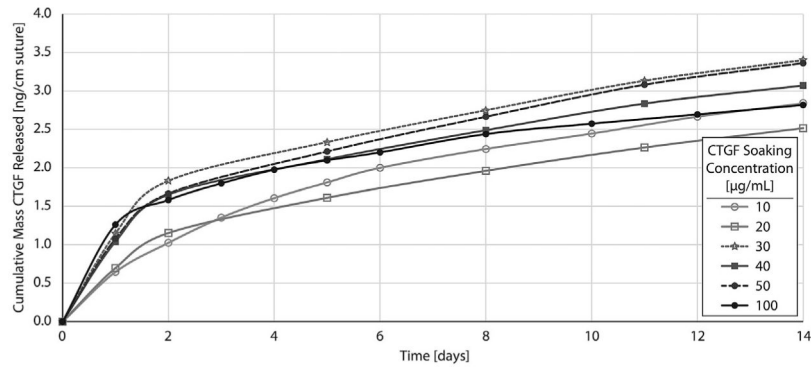


**Figure 4.** Cumulative CTGF release profiles for porous sutures loaded with a range of CTGF soaking concentrations (10–100 µg/ml) within a heparin/fibrin-based delivery system (HBDS), in vitro ( $n = 2$  per group, averaged). Porous sutures loaded with HBDS +CTGF showed an initial burst followed by sustained release over the first 14 days. The 30 µg/ml CTGF group was the highest loading concentration that did not form precipitate in solution.

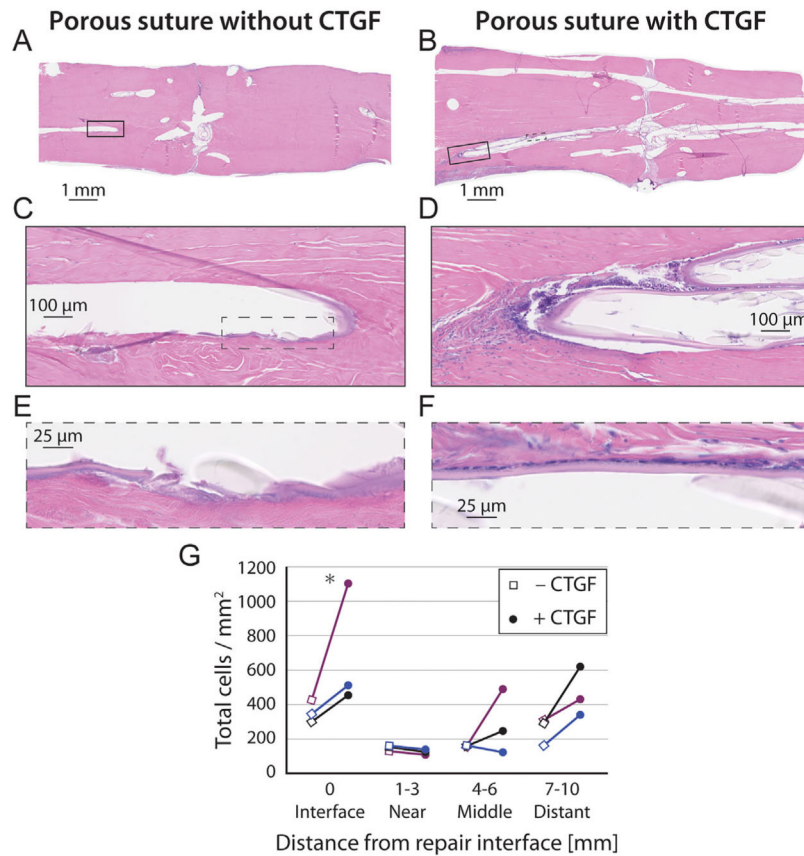


**Figure 5.** Histologic sections from canine FDP tendon 14 days after surgery with porous suture controls (A,C,E, no CTGF) or sutures containing CTGF (B,D,F), stained with H&E. (G) Normalized cell counts within 70 μm of the suture surface or within the repair interface region for paired samples. CTGF and position had significant effects on cell activity in the local region near the suture, as determined by 3-way ANOVA. \* $p < 0.05$  by Fisher's least significant difference post hoc analysis ( $n = 3$  per group).

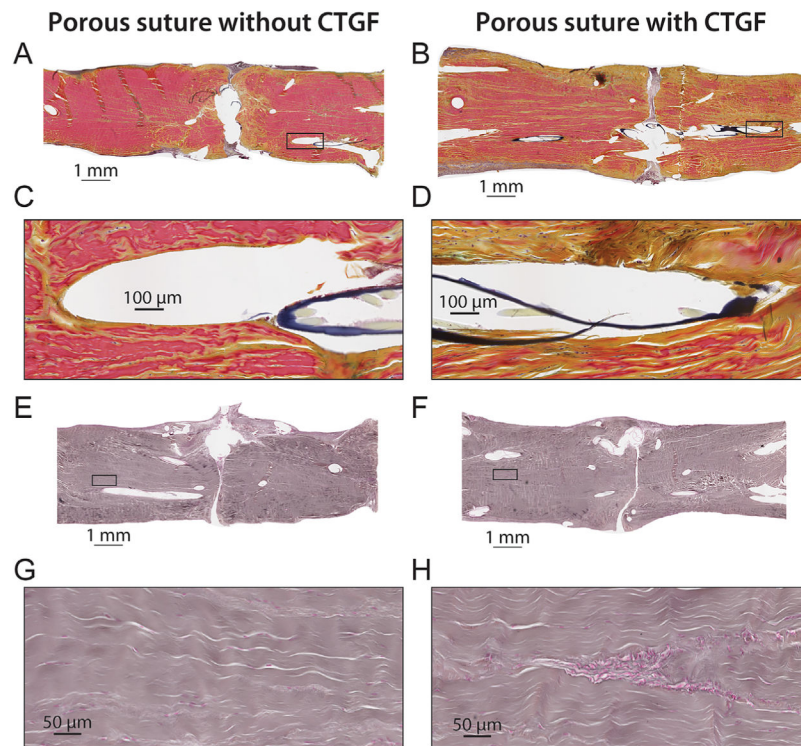


**Figure 6.** Histologic sections from canine FDP tendon 14 days after surgery with porous suture controls (A,C,E,G, no CTGF) or sutures containing CTGF (B,D,F,H), stained with pentachrome stain (A–D) or reticular stain (E–H). Tendons repaired with CTGF-laden sutures had increased staining for new collagen (yellow pentachrome stain) and evidence of likely capillary formation (reticular stain) throughout the tissue, especially adjacent to the suture. (H) The accumulation of cells in a cylindrical pattern in the tendon midsubstance is atypical for the avascular zone of flexor tendons, suggesting angiogenesis. (C,D,G,H) are 10× higher power views of the whole-tendon slides above them (A,B,E,F, respectively). Sections (A,E and B,F) were paired repairs from the same animal.

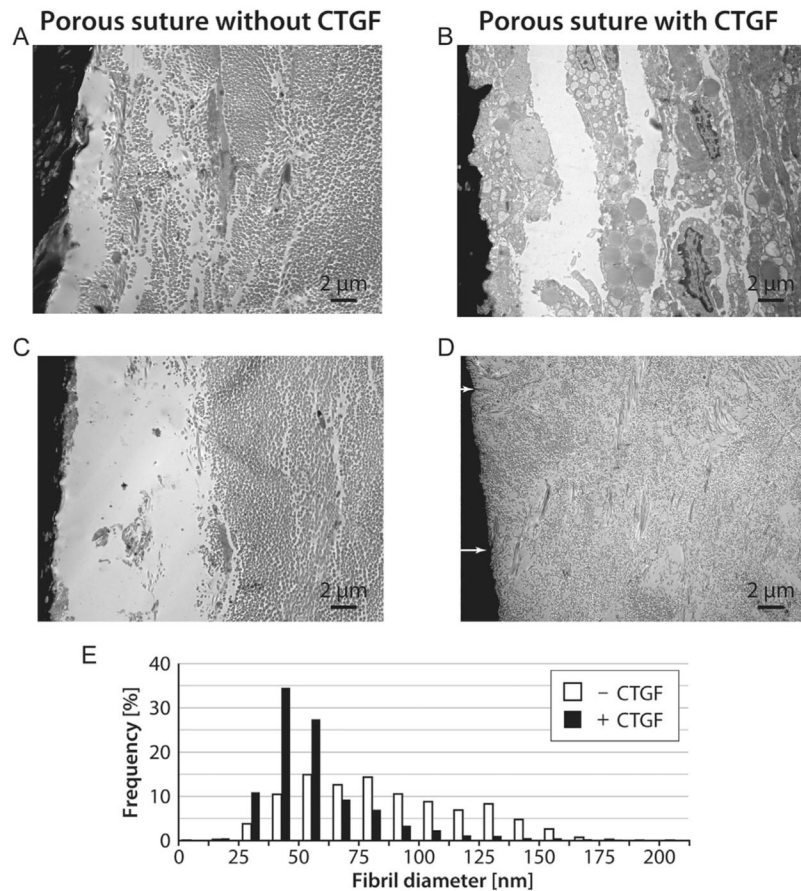


**Figure 7.** Transmission electron microscopy images of canine FDP tendon 14 days after surgery. Sutures appear black on the left side of each micrograph. (A,C) Porous suture controls lacking CTGF had large collagen fibrils and a clear glycoproteinaceous layer next to the suture. (B,D) CTGF-laden porous sutures induced increased cellular responses (B) and decreased collagen fibril size (D) compared to controls. White arrows indicate locations where collagen fibrils appear to enter the porous suture (D). (E) Histogram of collagen fibril diameters, combining  $n = 3$  representative TEM images per group. CTGF-laden porous sutures induced a 33% decrease in average fibril diameter surrounding the suture ( $p < 0.001$ ,  $n = 2$  tendons per group).

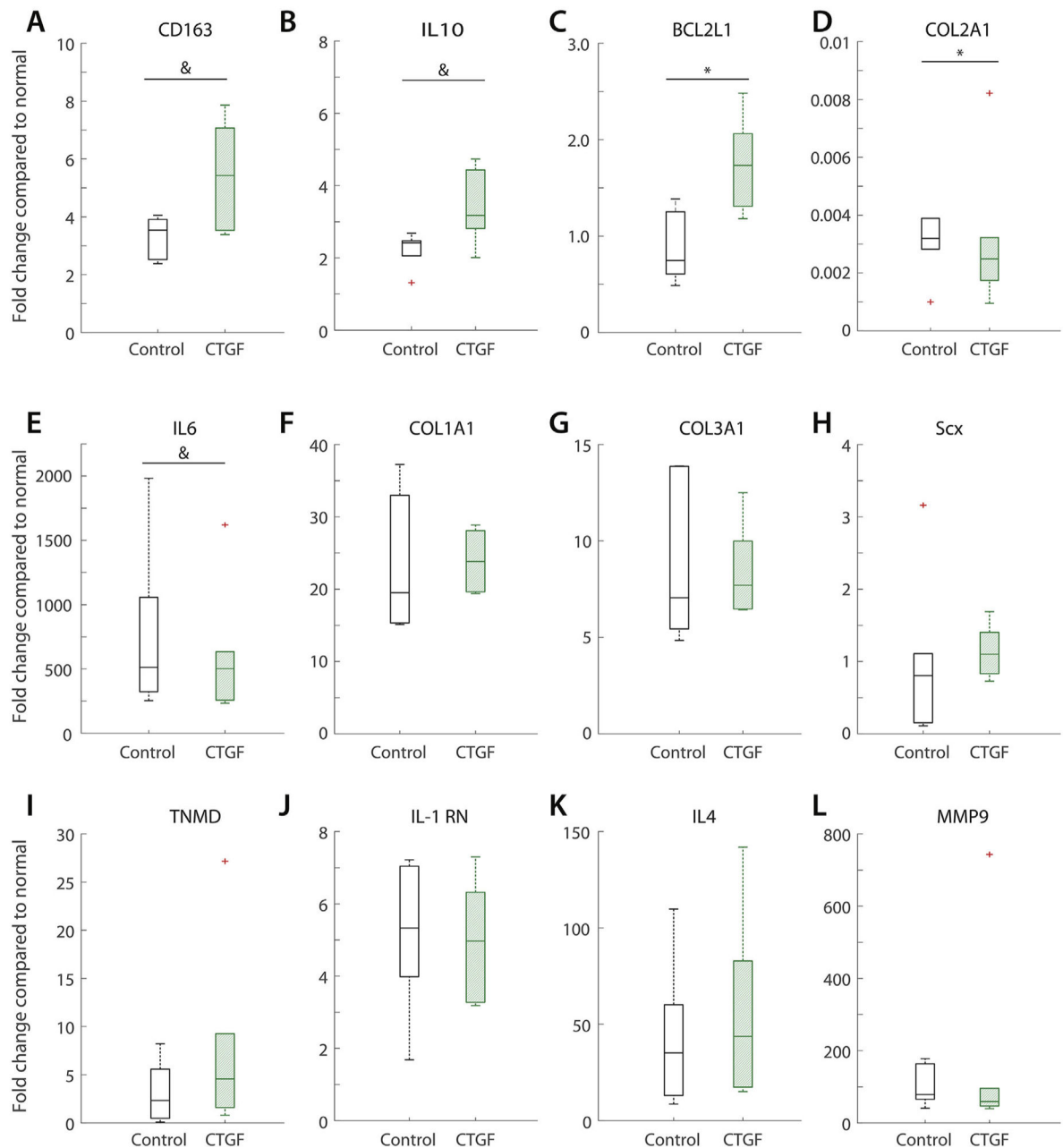


**Figure 8.**

Gene expression fold changes in repaired tendons using porous suture loaded with or without CTGF compared to normal, non-operated contralateral digits for (A) macrophage/monocyte marker *CD163*, (B) anti-inflammatory cytokine *IL10*, (C) anti-apoptotic factor *BCL2L1*, (D) extracellular matrix protein *COL2A1*, (E) cytokine *IL6*, extracellular matrix proteins (F) *COL1A1* and (G) *COL3A1*, tenogenic markers (H) *Scx* and (I) *TNMD*, cytokines (J) *IL1RN* and (K) *IL4*, and (L) matrix metalloproteinase *MMP9*. \*  $p < 0.05$ , &  $p < 0.1$  between groups by Wilcoxon signed-rank test ( $n = 6$  per group).

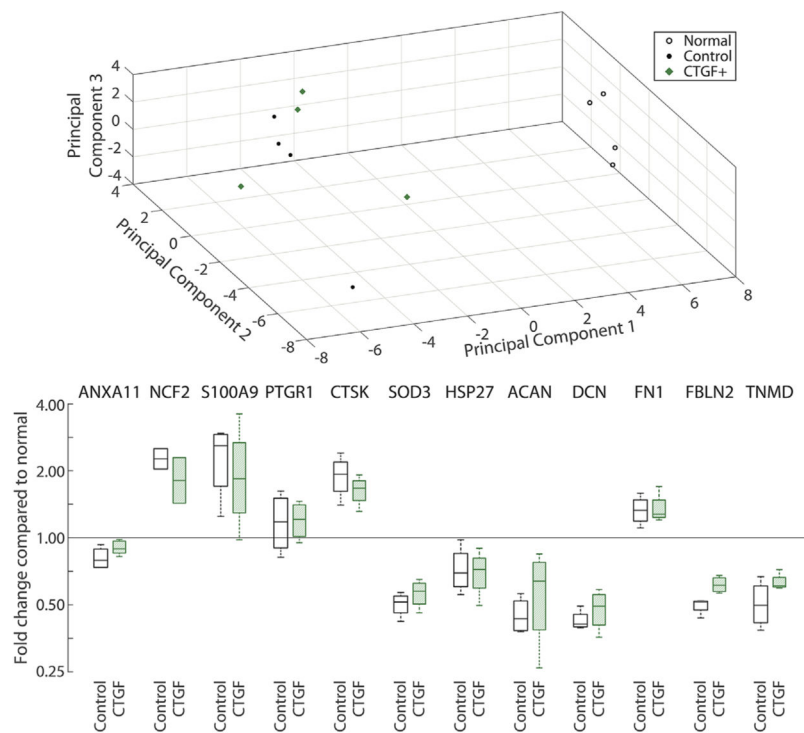


**Figure 9.** Protein expression principal component analysis (top) and fold changes compared to normal, non-operated contralateral digits (bottom, note log scale). Inflammatory proteins: ANXA11, annexin A11; NCF2, neutrophil cytosol factor 2; PTGR1, prostaglandin reductase 1; CTSK, cathepsin K, SOD3, superoxide dismutase 3; HSP27, heat shock protein 27. Extracellular matrix proteins: ACAN, aggrecan; DCN, decorin; FN1, fibronectin 1; FBLN2, fibulin 2. TNMD, tenomodulin. \*There were no significant differences in protein expression ( $n = 4$  per group).

**Table 1**

Precipitate Formation in Loading Buffer Containing Fibrinogen +CTGF/HBDS Components

<b>CTGF Soaking Concentration</b>	<b>Precipitate Formation</b>
10 µg/ml	No visible precipitate
20 µg/ml	
30 µg/ml	Very slight precipitate, disappeared within 1–2 s
40 µg/ml	Definite precipitate, disappeared after 5–10 s
50 µg/ml	Most, but not all, precipitate re-dissolved over time
100 µg/ml	Substantial precipitate did not re-dissolve

Author Manuscript

Author Manuscript

Author Manuscript

Author Manuscript